2020-02-29

Identification of multiple unknown point sources occurring in the 2D transport equation: application to groundwater pollution source identification

Soko, Alpha Omega

Journal of Mathematical and Computational Science

Identification of multiple unknown point sources occurring in the 2d transport equation: application to groundwater pollution source identification.

Article · January 2020

DOI: 10.28919/jmcs/4491

CITATION
1

READS
16

3 authors:

Alpha Soko
Pan African University Institute for Basic Sciences Technology and Innovation (PAUSTI)
4 PUBLICATIONS **0** CITATIONS
SEE PROFILE

Verdiana grace Masanja
The Nelson Mandela African Institute of Science and Technology
12 PUBLICATIONS **6** CITATIONS
SEE PROFILE

Jeconia Abonyo Okelo
Jomo Kenyatta University of Agriculture and Technology
11 PUBLICATIONS **5** CITATIONS
SEE PROFILE

Available online at http://scik.org

J. Math. Comput. Sci. 10 (2020), No. 4, 833-862

https://doi.org/10.28919/jmcs/4491

ISSN: 1927-5307

IDENTIFICATION OF MULTIPLE UNKNOWN POINT SOURCES OCCURRING IN THE 2D TRANSPORT EQUATION: APPLICATION TO GROUNDWATER POLLUTION SOURCE IDENTIFICATION

ALPHA OMEGA SOKO[1,*], VERDIANA GRACE MASANJA[2], OKELO JECONIAH ABONYO[3]

[1]Department of Mathematics, Pan African University Institute for Basic Sciences Technology and Innovation (PAUSTI), Nairobi, Kenya

[2]Nelson Mandela African Institution of Science and Technology (NM-AIST), Arusha, Tanzania

[3]Department of Pure and Applied Mathematics, Jomo Kenyatta University of Agriculture and Technology (JKUAT), Nairobi, Kenya

Abstract. Accessing quality water is of crucial importance to both society and the environment. Deterioration in water quality through groundwater pollution presents a substantial risk to human health, plant and animal life, and detrimental effects on the local economy. To ensure groundwater quality, there is need to identify locations of unknown groundwater pollution sources. In this paper, the locations of groundwater contaminant sources have been identified using inverse problem technique. The work in this paper concerns the inverse source problem in the Advection Dispersion Reaction Equation (ADRE) with an emphasis on groundwater pollution source identification. Mathematically, inverse source problem involves the reconstruction of the source function in the ADRE from the boundary and interior measurements. An inverse source problem technique for identifying the unknown groundwater pollution source utilizing only the boundary and interior measurements is developed. The finite volume discretization

*Corresponding author

E-mail address: alpha@aims.ac.tz

Received January 31, 2020

method is employed on the adjoint ADRE to provide the data. The data from the finite volume method results into Volterra integral equation which after discretizing transforms into an ill-posed inverse problem. Tikhonov regularization method is used to achieve stability on the ill-posed problem. The results indicates that our proposed inverse problem is accurate with the data.

Keywords: Tikhonov regularization; advection dispersion reaction equation; Volterra integral equation; pollution; inverse problem; groundwater.

2010 AMS Subject Classification: 35R30.

1. INTRODUCTION

The increasing rate of water resource usage results in their contamination by wastewater of domestic, industrial and agricultural sectors. Due to the increased need for freshwater, humans are opting for the groundwater reservoirs [14]. Thus there is a need to ensure quality groundwater for the sustenance of human health. To manage and supervise efficiently the groundwater quality in aquifers, accurate determination of the location and magnitude of pollution sources is necessary. The identification of pollution is done by monitoring the Biochemical Oxygen Demand (BOD) concentration which measures the amount of dissolved oxygen consumed by the microorganisms during the oxidation process [2].

BOD transport through groundwater is governed by the ADRE [4]. Identifying the sources of contamination from the spatial and temporal measurements of the BOD concentrations in the aquifer is an inverse problem which requires solving the ADRE backwards in time. Several approaches have been proposed in the last three decades to solve the ADRE backward in time to identify the contaminant sources in the groundwater. Mazaheri et al. (2015) [28], provided a comprehensive review of the available methodologies and classified them into three major groups; Simulation-optimization approach, Probabilistic approach and Mathematical approach.

The simulation-optimization approach has been employed by Mahar and Datta (2000) [26], who investigated pollution source locations in groundwater. Sequential unconstrained minimization technique was employed to solve the optimization problem. Recently, Huang et al. (2018) [20] used the simulation optimization approach by integrating numerical simulators MODFLOW and

MT3DMS into the grids traversal and shuffled complex evolution optimization algorithms in determining unknown pollution source from observed groundwater data. Despite the simplicity of formulation in the simulation-optimization approach, the computational cost is relatively high and the global optimum solution is not guaranteed and dealing with ill-posed conditions encountered in the approach is much more complicated.

In the probabilistic approach, statistical distributions are employed in model development. The most important feature of this approach is that the pollution source parameters are usually treated as random variables and probability distribution functions are used to predict them. Zeng et al. (2018)[23], used the backward probability method for characterizing the instantaneous pollutant source location and releasing time within a ventilation system. The physical problem was formulated in terms of a one-dimensional advection-diffusion model with branches and it was verified by the results of a purposely designed experiment. The backward method requires schemes which can stabilize the solution process and needs prior source information such as location. The backward method also has the limitation as it requires a limited number of pollution sources which has known locations. The information being required is usually difficult to obtain in physical applications.

In the mathematical approach, initially, the governing mass transfer equation is solved for each unit intensity pollution source independently. The final problem leads to a linear, ill-posed algebraic system of equations in which the intensities and locations of the pollution sources are unknown. The ill-posed condition is solved using regularization methods. Recently, Adel (2018) [1] used the mathematical approach in establishing a non-iterative method for identifying multiple unknown time-dependent sources compactly supported occurring in a 2D parabolic equation. It is noteworthy that the mathematics and formulation used in this method are relatively more complex with respect to the other methods but it is much less time-consuming.

The originality of the present study consists in addressing the linear inverse source problem of identifying multiple unknown time-dependent point sources occurring in a 2D ADRE with the solitary velocity profiles. Although the 2D mathematical model is subject to a lot of interest, the identification of multiple unknown time-dependent point sources in 2D evolution

transport equations remains an open problem. The paper is organized as follows: Section 2 is devoted to stating the problem, assumptions and proving some technical results for later use. In Section 3, we derive the adjoint differential equation which have been used in formulating the inverse problem. In Section 4, we establish an inverse problem identification method that uses the concentration records to compute the unknown source position and intensity function. Some numerical experiments done on a variant of groundwater pollution BOD are presented in Section 5.

2. Governing Equation and Problem Formulation

The model concerns the measurement of pollutant concentration by the use of BOD_5 values denoted herein by C. Let $\Omega \in \mathbb{R}^2$ be any connected and bounded open set with boundary $\partial\Omega$. The boundary $\partial\Omega$ is assumed to be of the form Equation (1).

$$\partial\Omega = \bigcup_{i=1}^{4} \Gamma_i \tag{1}$$

where Γ_1 represent the inflow boundary, Γ_4 represent the outflow boundary, Γ_2 and Γ_3 represents the lateral boundaries. Let Γ_L regroup the two lateral lower and upper boundaries as Equation (2):

$$\Gamma_L = \Gamma_2 \cup \Gamma_3 \tag{2}$$

Figure 1 depicts such set Ω with its boundaries.

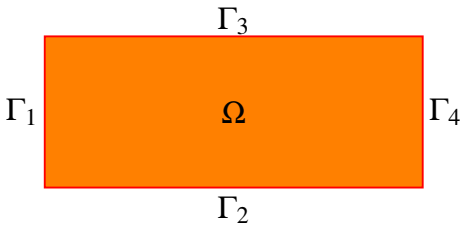

FIGURE 1. Boundary of the Polluted Aquifer

Let $T > 0$ be a final monitoring time. The BOD_5 is monitored within the time interval $(0, T)$. Thus the model is defined in the space $\Omega \times (0,\ T)$. The evolution of the BOD_5 concentration in

a porous medium is governed by the Equation (3) [31]:

$$\frac{\partial C}{\partial t} - \nabla \cdot (D\nabla C - \mathbf{V} \cdot C) + RC = F \tag{3}$$

where C is the pollutant concentration measured in mg/L, $\mathbf{V}$ is the flow velocity measured in m/s, R is the reaction coefficient measured in s^{-1} , F represents the set of all occurring pollution sources measured in $mgL^{-1}s^{-1}$ and D denotes the hydrodynamic dispersion tensor measured in m^2/s. Since Equation (3) is the equation for groundwater, it can be further simplified by applying the following assumptions; firstly, the groundwater is incompressible that is its density does not change when the pressure changes. Mathematically, this means that the density, ρ, of the groundwater is constant and therefore the continuity equation implies the Equation (4):

$$\frac{\partial \rho}{\partial t} + \nabla \cdot (\rho \mathbf{V}) = 0 \quad \Longleftrightarrow \nabla \cdot \mathbf{V} = 0 \tag{4}$$

secondly, $\mathbf{V}$ satisfies the no-slip boundary condition which means that along the lateral boundaries, the groundwater has zero velocity relative to the lateral boundary

$$\mathbf{V} = 0 \quad \text{on} \quad \Gamma_L \times (0, T) \tag{5}$$

Finally, the $\mathbf{V}$ satisfies the solitary vibrations of the Korteweg-de Vries equation (KdV) available on the interaction between groundwater and surface water. Thus the velocity $\mathbf{V} = (v_1, v_2)^T$ is a spatial-temporal varying field that satisfies the Equation (6):

$$\left.\begin{aligned} \frac{\partial v_1}{\partial t} + 6v_1\frac{\partial v_1}{\partial x} + \frac{\partial^3 v_1}{\partial x^3} &= 0 \\ \frac{\partial v_2}{\partial t} + 6v_2\frac{\partial v_2}{\partial y} + \frac{\partial^3 v_2}{\partial y^3} &= 0 \end{aligned}\right\} \quad \text{in} \quad \Omega \tag{6}$$

The Equation (6) is to model groundwater flow velocity which is independent of the pollution concentrations. For detailed derivations for the velocity profile see [21, 30]. Simplifying Equation (3) using the Equation (4) gives the Equation (7);

$$\frac{\partial C}{\partial t} + \mathbf{V} \cdot \nabla C - \nabla \cdot (D\nabla C) + RC = F(x,t) \tag{7}$$

Hydrodynamic dispersion refers to the stretching of a solute band in the flow direction during its transport by an advecting fluid [32]. It occurs as a consequence of two processes; molecular diffusion which results from the random molecular motion and mechanical dispersion which is caused by non-uniform velocities. With these two processes the hydrodynamic dispersion is given by the Equation (8):

$$D = \begin{pmatrix} D_{xx} & D_{xy} \\ D_{yx} & D_{yy} \end{pmatrix} \tag{8}$$

where the spatially varying entries $D_{xx}, D_{yy}, D_{xy}, D_{yx}$ satisfy the Equations (9) to (11) [4, 27]:

$$D_{xx} = \frac{a_L v_1^2 + a_T v_2^2}{||\mathbf{V}||^2} \tag{9}$$

$$D_{yy} = \frac{a_T v_1^2 + a_L v_2^2}{||\mathbf{V}||^2} \tag{10}$$

$$D_{xy} = \frac{(a_L - a_T)\, v_1 v_2}{||\mathbf{V}||^2} = D_{yx} \tag{11}$$

Where a_T and a_L are the transverse and longitudinal dispersion coefficients respectively and $||\cdot||$ is the usual Euclidean norm. For the reaction coefficient, R, we use the linear model due to Dobbins (1964)[10], that combines groundwater de-oxygenation rate and groundwater sedimentation rate as in the Equation (12);

$$R([BOD]) = (K_d + K_s)\,[BOD] \tag{12}$$

where K_d, K_s are the de-oxygenation and sedimentation rate respectively.

The major challenge for an inverse problem regarding the identification of a function source F in the Equation (7) is the fact that F cannot be uniquely determined in its general form. For instance, let $f \in \mathscr{D}(\Omega)$ be an infinity differentiable function with compact support in Ω and $g = -\nabla^2 f$. Then $v(x,y,t) = tf(x,y)$ satisfies the Equations (13) to (15):

$$\frac{\partial v}{\partial t} - \nabla^2 v = f + tg \quad \text{in} \quad \Omega \times (0,T) \tag{13}$$

$$v(\cdot, 0) = 0 \quad \text{in} \quad \Omega \tag{14}$$

$$\nabla v \cdot \nu = 0 \quad \text{on} \quad \partial\Omega \times (0, T) \tag{15}$$

Without having necessarily $f + tg$ null [11]. Therefore, the same boundary records may lead to the identification of different sources. This means that for a well-posed inverse source problem a priori information on the sources should be available. Hamdi (2017) noted that the information takes the form of some conditions on the admissible sources [18]. Yamamoto (1993) considered sources of the form $F(x,t) = \alpha(t)f(x)$ where $f \in L^2$ and the time-dependent function $\alpha \in C^1([0,T])$ was assumed to be known and satisfying the condition $\alpha(0) \neq 0$ [35]. Time-independent sources $F(x,t) = f(x)$ are treated by Cannon (1968) using spectral theory [8]. In this paper, point sources of the Equation (16):

$$F(\mathbf{x},t) = \sum_{i=1}^{Ns} w_i(t)\delta(\mathbf{x} - \mathbf{S}_i) \tag{16}$$

are considered. In Equation (16), w_i is the ith source intensity function, δ is the Dirac delta function, $\mathbf{S}_i$ is the ith source location.

For the initial condition, without loss of generality, the assumption that no pollution occurs at the initial monitoring time is reasonable since at this time the pollutant has yet to mix with the water. Thus a null initial BOD concentration. Since the pollutants are introduced on the boundaries and as the convective transport generally dominates the diffusion process,an assumption that no pollution concentration on the inflow boundary is reasonable. Finally, a null gradient concentration at the downstream boundary which represent no variation in BOD concentration. Therefore, given the Equation (7), the BOD_5 concentration C satisfies the Equations (17) to (19):

$$\frac{\partial C}{\partial t} + \mathbf{V} \cdot \nabla C - \nabla \cdot (D\nabla C) + RC = \sum_{i=1}^{Ns} w_i(t)\delta(\mathbf{x} - \mathbf{S}_i) \quad \forall (\mathbf{x},t) \in \Omega \times (0,T) \tag{17}$$

$$C(x,y,0) = 0 \quad \text{in} \quad \Omega \tag{18}$$

$$C(x,y,t) = 0 \quad \text{on} \quad \Gamma_1 \times (0,T) \tag{19}$$

$$\nabla C(x,y,t) = 0 \quad \text{on} \quad (\Gamma_L \cup \Gamma_4) \times (0,T) \tag{20}$$

The problem in the Equations (17) to (19) admits a unique solution C that belongs to the functional space in the Equation (21) [1, 25]:

$$L^2\left(0,T;L^2(\Omega)\right)\cap\mathscr{C}(0,T;H^{-1}(\Omega)) \tag{21}$$

As the source position $\mathbf{S}_i$ is assumed to be in the interior of the domain Ω, the state C is smooth on the boundary $\partial\Omega$, which allows defining the boundary observation operator in the Equation (22):

$$M[F] := \{C(a,t), C(b,t) \quad \text{for} \quad 0<t<T\} \tag{22}$$

where a and b are observation points satisfying $0 < a < b < l$. This is called a direct problem. The inverse problem the paper is dealing with is; assuming available the records $\{d_a(t),\ d_b(t)\,\text{for} \quad 0<t<T\}$ of the concentration C at the two observation points a and b, find the source F satisfying the observation in the Equation (23):

$$M[F] = \{d_a(t), d_b(t) \quad for \quad 0<t<T\} \tag{23}$$

Before proceeding, we need to show that if two measured concentrations of BOD coincide on Γ_4, then they are generated by the same source. This allows us to know whether the inverse problem is well-posed and whether the solution to the problem is indeed that of the inverse problem. This result is given in Theorem 2.2. As part of the requirement for the proof of the Theorem 2.2, we establish the unique continuation property. For a general differential operator, L and state function u, the unique continuation property asserts that a solution of an equation $Lu = 0$ in a domain which vanishes in an open subset vanishes identically.

Lemma 2.1. Let $Ns \in \mathbb{N}$ be an unknown number of sources. Assume that the source positions $\mathbf{S}_i$ for $i = 1, 2, \ldots Ns$ are distinct and the intensity functions $w_i(t) \in L^2(0,T)$ are all positive functions. Consider the initial boundary value problem in the Equations (24) to (26):

$$\frac{\partial C}{\partial t} + \mathbf{V}\cdot\nabla C - \nabla\cdot(D\nabla C) + RC = \sum_{i=1}^{Ns} w_i(t)\delta(\mathbf{x}-\mathbf{S}_i) \quad \forall(\mathbf{x},t)\in\Omega\times(0,T) \tag{24}$$

$$C(x,y,0) = \psi_1 \quad \text{in} \quad \Omega \tag{25}$$

$$C(x,y,t) = \psi_2 \quad \text{on} \quad \Gamma_L\times(0,T) \tag{26}$$

where $\psi_1 \in H^1(\Omega)$, $\psi_2 \in H^s(\Gamma_L)$ satisfying the compatibility condition $\psi_1 = \psi_2$ on Γ_L. Then $C(x, y, t) = 0 \quad \text{on} \quad \Gamma_L$ only if $w_i(t)$ are null.

Proof. We recall the unique continuation theorem of Mizohata [34]: If Ω is a connected open set in $\mathbb{R}^2$, ω an open subset of Ω and if, $C \in L^2\left(0, T; H^2_{\text{loc}}(\Omega)\right)$, verifies the Equations (27) and (28):

$$\frac{\partial C}{\partial t} + \mathbf{V} \cdot \nabla C - \nabla \cdot (D \nabla C) + RC = 0 \quad \forall (\mathbf{x}, t) \in \Omega \times (0, T) \tag{27}$$

$$C(x, y, t) = 0 \quad \text{in} \quad \omega \times (0, T) \tag{28}$$

then $C(x, y, t) = 0 \quad \text{on} \quad \Omega \times (0, T)$ □

Theorem 2.2. Let $Ns \in \mathbb{N}$ be an unknown number of sources. Assume that the source positions $\mathbf{S}_i$ for $i = 1, 2, \ldots Ns$ are distinct and the intensity functions $w_i(t) \in L^2(0, T)$ are all positive functions. The source function in the Equations (17) to (19):

$$F(\mathbf{x}, t) = \sum_{i=1}^{Ns} w_i(t) \delta(\mathbf{x} - \mathbf{S}_i)$$

is uniquely determined by the observation Equation (23).

Proof. Let C_j for $j = 1, 2$ be the solutions to the Equations (17) to (19) with the time dependent point source in the Equation (29):

$$F_j(x, t) = \sum_{i=1}^{Ns} w_i^j(t) \delta(\mathbf{x} - \mathbf{S}_i^j) \tag{29}$$

and the same observation Equation (23). Assume that $M(F_1) = M(F_2)$, we have to prove that $F_1 = F_2$. Denote by φ the difference $C_2 - C_1$. Clearly φ satisfies the system of Equations (30) to (33):

$$\frac{\partial \varphi}{\partial t} + \mathbf{V} \cdot \nabla \varphi - \nabla \cdot (D \nabla \varphi) + R\varphi = F_2 - F_1 \quad \forall (\mathbf{x}, t) \in \Omega \times (0, T) \tag{30}$$

$$\varphi(x, y, 0) = 0 \quad \text{in} \quad \Omega \tag{31}$$

$$\varphi(x, y, t) = 0 \quad \text{on} \quad \Gamma_1 \times (0, T) \tag{32}$$

$$\nabla \varphi(x, y, t) = 0 \quad \text{on} \quad (\Gamma_L \cup \Gamma_4) \times (0, T) \tag{33}$$

Let $\mathscr{B} \subset \mathbb{R}^2$ be an open disk such that $(\mathscr{B} \cap \partial\Omega) \subset \Gamma_4$. Since the points $\mathbf{S}_i$ for $i = 1, 2, \ldots Ns$ are in the interior of Ω, we choose $\mathscr{B}$ such that and $\mathbf{S}_i^j \notin \overline{\mathscr{B}}$ for $j = 1, 2$. Therefore the open $\Pi_1 = (\mathscr{B} \cap \Omega) \subset \Omega \backslash \{S^j\}$. The condition $C(x, y, t) = 0 \quad \text{on} \quad \mathscr{B} \cap \Gamma_L$ permits to deduce that the extension of φ by zero in $\Pi_2 \times (0, T)$ where $\Pi_2 = \mathscr{B} \cap (\mathbb{R}^2 \backslash \overline{\Omega})$, is a solution of the Equations (34) and (35):

$$\frac{\partial \varphi}{\partial t} + \mathbf{V} \cdot \nabla \varphi - \nabla \cdot (D \nabla \varphi) + R\varphi = 0 \quad \forall (\mathbf{x}, t) \in \mathscr{B} \times (0, T) \tag{34}$$

$$\varphi(x, y, t) = 0 \quad \text{on} \quad \Pi_2 \times (0, T) \tag{35}$$

Thus according to Lemma 2.1 $\varphi = 0 \quad \text{in} \quad \Pi_1 \times (0, T)$. A second application of Lemma 2.1 in $(\Omega \backslash \{S^j\}) \times (0, T)$ instead of $\Omega \times (0, T)$ yields the Equation (36):

$$\varphi = 0 \quad \text{in} \quad (\Omega \backslash \{S^j\}) \times (0, T) \tag{36}$$

Then, since $\varphi \in L^2(\Omega \times (0, T))$ it follows that $\varphi = 0$ in $\Omega \times (0, T)$. This implies that $F_1 = F_2$. $\square$

3. Greens Function Method to Solve Direct Problem

Let $\hat{\mathbf{n}}$ be an outward normal of unit length to the space Ω. The non-homogeneous Equation (17) is equivalent to the Equation (37):

$$\mathscr{L} C(\mathbf{x}) = f(\mathbf{x}), \tag{37}$$

where $\mathbf{x}$ is a vector in more than one dimension, $\mathscr{L}$ is a linear partial differential operator in more than one independent variables given by the Equation (38)

$$\mathscr{L} C(\mathbf{x}) = \frac{\partial C(\mathbf{x})}{\partial t} + \mathbf{V} \cdot \nabla C(\mathbf{x}) - \nabla \cdot (D \nabla C(\mathbf{x})) + RC(\mathbf{x}) \tag{38}$$

$f(\mathbf{x})$ is the right-hand side of Equation (17). The Green's function for Equation (37) will be obtained from using the Greens identity which gives the relationship between the operator, $\mathscr{L}$, and its Adjoint Operator $\mathscr{L}^*$. For an arbitrary test function, $g(\mathbf{x})$ and an independent number of the variables N, the fundamental relation which defines the adjoint operator $\mathscr{L}^*$ is given by the

Equation (39) [22];

$$g(\mathbf{x})\mathscr{L}C(\mathbf{x}) - C(\mathbf{x})\mathscr{L}^* g(\mathbf{x}) = \sum_{\alpha=1}^{N} \frac{\partial}{\partial x_\alpha} M_\alpha(C, g) \tag{39}$$

where function $M(C, g)$ is a boundary term which involves the values of $C(\mathbf{x})$, $g(\mathbf{x})$, and some of their partial derivatives on the boundary. Multiply the Equation (39) by the volume element $\mathrm{d}\sigma$ on both sides then integrate over Ω and on the right side apply, the Gaussian integral transformation in the Equation (40):

$$\int_{\Omega} \sum_{\alpha=1}^{N} \frac{\partial}{\partial x_\alpha} M_\alpha(C, G)\, \mathrm{d}\sigma = \int_{\partial\Omega} \sum_{\alpha=1}^{N} \frac{\partial}{\partial x_\alpha} M_\alpha(C, g)\hat{\mathbf{n}}\, \mathrm{d}\sigma \tag{40}$$

where $\hat{\mathbf{n}}$ is the outside normal of the boundary surface $\partial\Omega$. After integration, the Equation (39) gives the Equation (41):

$$\int_0^T \int_{\Omega} [g(\mathbf{x})\mathscr{L}C(\mathbf{x}) - C(\mathbf{x})\mathscr{L}^* g(\mathbf{x})]\, \mathrm{d}\sigma \mathrm{d}\eta = \int_0^T \int_{\partial\Omega} \sum_{\alpha=1}^{N} \frac{\partial}{\partial x_\alpha} M_\alpha(C, g)\hat{\mathbf{n}}\, \mathrm{d}\sigma \mathrm{d}\eta \tag{41}$$

In the search for the Green's function, the starting point in the solution of Equation (37) by the method of Green's function, is the Equation (41) with g substituted by G, which is the Green's function. Substituting the integration variables $\mathbf{x}$ by the dummy variables ξ, gives the Equation (42):

$$\int_0^T \int_{\Omega} G\mathscr{L}_\xi C\, \mathrm{d}\sigma_\xi \mathrm{d}\eta = \int_0^T \int_{\partial\Omega} \sum_{\alpha=1}^{N} \frac{\partial}{\partial \xi_\alpha} M_\alpha(C, G)\hat{\mathbf{n}}\, \mathrm{d}\sigma_\xi \mathrm{d}\eta + \int_0^T \int_{\Omega} C\mathscr{L}^* G\, \mathrm{d}\sigma_\xi \mathrm{d}\eta \tag{42}$$

Where $\mathrm{d}\sigma_\xi$ is the new volume element resulting from the variable change. The boundary terms in Equation (42) and $\mathscr{L}_\xi^*$ are found by carrying out the integration by parts of the left-hand side with the given operator $\mathscr{L}_\xi$. At the same time, $\mathscr{L}_\xi C = f(\xi)$, this gives the Equation (43);

$$\mathscr{L}^* G = -\frac{\partial G}{\partial t} - \mathbf{V}\cdot\nabla G - \nabla\cdot D\nabla G + RG \tag{43}$$

The boundary terms are given by the Equation (44):

$$\int_0^T \int_{\partial\Omega} \sum_{\alpha=1}^{N} \frac{\partial}{\partial \xi_\alpha} M_\alpha(C,G)\cdot\hat{\mathbf{n}}\,\mathrm{d}\sigma_\xi\,\mathrm{d}\eta = \int_0^T \int_{\partial\Omega} CG\cdot\hat{\mathbf{n}}\,\mathrm{d}\sigma_\xi\,\mathrm{d}\eta + \int_0^T \int_{\partial\Omega} G\,(\mathbf{V}C - D\nabla C)\cdot\hat{\mathbf{n}}\,\mathrm{d}\sigma_\xi\,\mathrm{d}\eta$$

$$+ \int_0^T \int_{\partial\Omega} C\,(D\nabla G)\cdot\hat{\mathbf{n}}\,\mathrm{d}\sigma_\xi\,\mathrm{d}\eta \tag{44}$$

Depending on the choice of G, Equation (42) provides the solution to the original problem. Specifically, if, G, satisfies the Equation (45):

$$\mathscr{L}^* G = \delta(\mathbf{x}-\xi)\delta(t-\tau) \tag{45}$$

Then the last term in Equation (42) is simply $C(\mathbf{x})$. The boundary conditions of Equation (45) are obtained also from Equation (44). Applying boundary conditions, Equations (18) to (20) on the Equation (44) gives the Equation (46):

$$\int_0^T \int_{\partial\Omega} \sum_{\alpha=1}^{N} \frac{\partial}{\partial \xi_\alpha} M_\alpha(C,G)\cdot\hat{\mathbf{n}}\,\mathrm{d}\sigma_\xi\,\mathrm{d}\eta = \int_0^T \int_{\Gamma_L\cup\Gamma_4} C(G + D\nabla G + GV)\cdot\hat{\mathbf{n}}\,\mathrm{d}\sigma_\xi\,\mathrm{d}\eta$$

$$- \int_0^T \int_{\Gamma_1} GD\nabla C\cdot\hat{\mathbf{n}}\,\mathrm{d}\sigma_\xi\,\mathrm{d}\eta \tag{46}$$

Since ∇C is non-zero on the boundary Γ_1, it suffices that $G = 0$ on Γ_1. Similarly, as C is non zero on the boundary Γ_L, then $\nabla G = 0$ on Γ_L. Finally, as C is non-zero on the boundary Γ_4 then $G = 0$ on Γ_4. We summarize this in the Definition 3.1:

Definition 3.1. The Green's function $G(\mathbf{x}, t; \xi, \tau)$ of operator $\mathscr{L}$ is the unique solution of the problem in the Equations (47) to (50):

$$\mathscr{L}^* G = \delta(\mathbf{x}-\xi)\delta(t-\tau) \tag{47}$$

$$G(x,y,0;\xi,\tau) = 0 \quad \text{in} \quad \Omega\times(0,T) \tag{48}$$

$$G(x,y,t;\xi,\tau) = 0 \quad \text{on} \quad (\Gamma_1\cup\Gamma_4)\times(0,T) \tag{49}$$

$$\nabla G(x,y,t;\xi,\tau) = 0 \quad \text{on} \quad \Gamma_L\times(0,T) \tag{50}$$

The Greens function represents the effect at the point $\mathbf{x}$ of the Dirac delta function source at the point (ξ, τ). With the Green's function satisfying Equations (47) to (50) the left-hand side of Equation (42) is just the integral of the greens function multiplied by the function f. Thus the solution of Equation (37) is given by the Equation (51):

$$C(\mathbf{x}) = \int_0^T \int_\Omega G(\mathbf{x}, t; \xi, \tau) f(\xi, \tau) \mathrm{d}\xi \mathrm{d}\tau \tag{51}$$

The whole point of this method is that the Boundary Value Problem (BVP) governing G is generally simpler than the original governing C.

4. Method for Solving the Inverse Problem

4.1. Identification of the unknown source intensity function. The greens function in Equation (51) is obtained by solving Equation (47) in conjunction with the initial and boundary conditions in Equations (48) to (50) by the Finite Volume Method (FVM) (central spatial discretization and Crank-Nicolson time integration scheme). Making substitution of $f(\xi, \tau)$ in Equation (51), the solution is given by the Equation (52):

$$C(\mathbf{x}) = \int_0^T \int_\Omega G(\mathbf{x}, t; \xi, \tau) \sum_{i=1}^{Ns} w_i(\tau) \delta(\xi - \mathbf{S}_i) \mathrm{d}\xi \mathrm{d}\tau \tag{52}$$

Simplifying Equation (52) by taking the summation out of the integral sign and applying the shifting property of the delta function gives the Equation (53):

$$C(\mathbf{x}) = \sum_{i=1}^{Ns} \int_0^T w_i(\tau) G(\mathbf{x}, t; \xi, \tau) \mathrm{d}\tau \tag{53}$$

The greens function in Equation (53) must be computed for each point source on the various sources Ns using the FVM method. Using Equation (53), the concentration of the ith source point located at $\mathbf{x}_s$, is given by the Equation (54):

$$C(\mathbf{x}) = \int_0^T w(\tau) G(\mathbf{x}, t; \mathbf{x}_s, \tau) \mathrm{d}\tau \tag{54}$$

where $w(\tau)$ is the intensity function of the source. Equation (54) represents the linear Volterra Integral Equation of the First Kind (VIEFK). To solve Equation (54) in an interval $[0, b]$, divide the interval into smaller intervals of width h. Denote by $\mathbf{x}_i$, the point of subdivision such that $\mathbf{x}_i = ih$, for $i = 0, 1, 2, \ldots, m$ and $mh = b$. The left hand-side of Equation (54), $C(\mathbf{x})$, is known from FVM of the Equations (17) to (19) and is calculated at the finite number of points $\mathbf{x}_1, \mathbf{x}_2, \ldots, \mathbf{x}_m$. The Greens function is calculated from Equation (47) on the points $\mathbf{x}_s = \mathbf{x}_1, \mathbf{x}_2, \ldots, \mathbf{x}_m$. Furthermore, $w(\tau)$ is the only unknown that should be calculated to identify the pollution source. In-order to discretize Equation (54), the rectangular method is employed [24, 3]. On this method, an assumption that the averages of the intensities of the source for the points $\mathbf{x}_s = \mathbf{x}_1, \mathbf{x}_2, \ldots, \mathbf{x}_m$ are given by $w_1, w_2, \ldots, w_m$ respectively, changes Equation (54) into the Equation (55):

$$C(\mathbf{x}_j) = \int_0^T w_i(\tau) G(\mathbf{x}_j, t; \mathbf{x}_s, \tau) \mathrm{d}\tau \tag{55}$$

The integral in the Equation (55) is then approximated by Equation (56):

$$C(\mathbf{x}_j) = h \sum_{i=1}^{m} G(\mathbf{x}_j, t_i; \mathbf{x}_s, \tau) w_i \quad \text{for} \quad j = 1, 2, \ldots, m \tag{56}$$

Equation (56) introduces the relationship between the measured concentration $C(\mathbf{x}_1)$ in the groundwater and the pollution source at $\mathbf{x} = \mathbf{x}_s$. Similarly, if the concentrations corresponding to times $t_2, t_3, \ldots, t_n$ are $C(\mathbf{x})_2, C(\mathbf{x}_3), \ldots C(\mathbf{x}_n)$ respectively, then the system of linear algebraic equations in the Equation (57) is obtained:

$$\mathbf{G}\mathbf{w} = \mathbf{C} \tag{57}$$

where:

$$\mathbf{G} = \begin{pmatrix} G_{11} & G_{12} & \ldots & G_{1m} \\ G_{21} & G_{22} & \ldots & G_{2m} \\ \vdots & \vdots & \ldots & \vdots \\ \vdots & \vdots & \ldots & \vdots \\ G_{n1} & G_{n2} & \ldots & G_{nm} \end{pmatrix}, \quad \mathbf{w} = \begin{pmatrix} w_1 \\ w_2 \\ \vdots \\ \vdots \\ w_m \end{pmatrix}, \quad \mathbf{C} = \begin{pmatrix} c_1 \\ c_2 \\ \vdots \\ \vdots \\ c_m \end{pmatrix} \tag{58}$$

The system in Equation (57) is extended to Ns sources occurring in multiple locations, N_p concentration-time measurements in the groundwater to produce the Equation (59):

$$\begin{pmatrix} Q_{11} & Q_{12} & \dots & Q_{1m} \\ Q_{21} & Q_{22} & \dots & Q_{2m} \\ \vdots & \vdots & \dots & \vdots \\ \vdots & \vdots & \dots & \vdots \\ Q_{n1} & Q_{n2} & \dots & Q_{nm} \end{pmatrix} \begin{pmatrix} R_1 \\ R_2 \\ \vdots \\ \vdots \\ R_m \end{pmatrix} = \begin{pmatrix} U_1 \\ U_2 \\ \vdots \\ \vdots \\ U_m \end{pmatrix} \tag{59}$$

The System in the Equation (59) is a block system in which every element of the matrix is a matrix and every element of the vectors is a vector, that is, Q_{ij} for $1 \leq i \leq N_s$ and $1 \leq j \leq N_p$, is the coefficients matrix associated with the jth measurement point and the ith source, R_i for $1 \leq i \leq N_s$, is the vector of unknown average intensities of the ith source and U_j for $1 \leq j \leq N_p$ is the vector that represents concentration versus time at the jth measurement point.

The number of equations in Equation (59) should be equal to or greater than the number of unknowns to be able to find a solution. In the latter case, the system of equations is over-determined and can be solved using the linear least-squares method; however, the problem of source identification, encountered in this problem is ill-posed as it does not satisfy the well-posedness conditions of Hadamard [17]. According to [17] an ill-posed problem is the one that at least has one of these conditions: (i) nonexistence of answer, (ii) non-uniqueness of answer and (iii) no continuous relationship between input and output. In this case conditions (i) and (ii) are satisfied but not condition (iii) because of lack of stability of the system. To solve the ill-posed system, Tikhonov Regularization Method (TRM) is used to convert the ill-posed system to well-posed system. This is described in Section 4.2.

4.2. Tikhonov Regularization of the Inverse Problem. This section examines the solution of the linear system of equations from Equation (57) using the TRM. For convenience, Equation (57) is rewritten into Equation (60);

$$\mathbf{Gw} = \mathbf{C}, \quad \mathbf{G} \in \mathbb{R}^{m \times n}, \quad \mathbf{w}, \mathbf{C} \in \mathbb{R}^m \tag{60}$$

Since the entries of $\mathbf{C}$ are obtained through observation, they typically are contaminated by measurement errors and discretization errors. Let $\mathbf{e} \in \mathbb{R}^m$ be the sum of all the errors. Decompose the BOD concentration data, C, into the sum of error-free data, $\mathbf{c}_0 \in \mathbb{R}^m$, and the errors due to measurements and discretization in the Equation (61):

$$\mathbf{C} = \mathbf{c}_0 + \mathbf{e} \tag{61}$$

Let, $\mathbf{w}_0$, be the solution to the error-free linear system in the Equation (62). Since the vector $\mathbf{c}_0$ contains no perturbations and the matrix $\mathbf{G}$ is not ill-conditioned, it follows that the linear system Equation (62);

$$\mathbf{G}\mathbf{w}_0 = \mathbf{c}_0, \quad \mathbf{G} \in \mathbb{R}^{m\times n}, \quad \mathbf{w}_0, \mathbf{c}_0 \in \mathbb{R}^2 \tag{62}$$

is consistent. Let, $\mathbf{G}^{-1}$, denote the inverse matrix of $\mathbf{G}$. We are interested in computing an approximation of the solution, $\mathbf{w}_0 = \mathbf{G}^{-1}\mathbf{c}_0$, of the error-free linear system, Equation (62), by determining an approximate solution of the error-contaminated linear system, Equation (60). Direct computation of the solution of the Equation (60), gives the Equation (63):

$$w = \mathbf{G}^{-1}(\mathbf{c}_0 + \mathbf{e}) = \mathbf{w}_0 + \mathbf{G}^{-1}\mathbf{e} \tag{63}$$

which is meaningless as it is dominated by the propagated error. Tikhonov regularization seeks to determine an approximation of w_0 by minimizing the quadratic functional in Equation (64) [5, 6, 7, 13]:

$$\min_{\mathbf{w}\in\mathbb{R}^2} \left\{ ||\mathbf{G}\mathbf{w} - \mathbf{C}||^2 + \lambda^2 ||\Gamma\mathbf{w}||^2 \right\} \tag{64}$$

where λ is a constant chosen to control the size of the solution vector, and $\Gamma \in \mathbb{R}^{k\times n}$, $k \leq n$, is the regularization matrix. The operator $||\cdot||^2$ represents the Euclidean norm. Since the desired solution, $\mathbf{w}_0$, has known properties, then according to [5], Γ has to be chosen as a scaled finite difference approximation of order equal to the order of the equation [29, 33]. Thus the regularization matrix is the tri-diagonal second-order finite difference approximation in the

Equation (65)

$$\Gamma = \begin{pmatrix} -2 & 1 & & & \\ 1 & -2 & 1 & & \\ & 1 & \ddots & \ddots & \\ & & \ddots & \ddots & 1 \\ & & & 1 & -2 \end{pmatrix} \tag{65}$$

It is well known that the solution $\mathbf{w}_\lambda$ to the Equation (64) solves the Equation (66) [16]:

$$\left(G^T G + \lambda \Gamma^T \Gamma\right) w = G^T C \tag{66}$$

From Equation (66), note that if λ is close to zero, then due to the ill-conditioning, $\mathbf{w}$ is badly computed. On the other hand, if λ is far away from zero, $\mathbf{w}$ is well computed but the error $w - w_0$ is quite large. Thus, the choice of a good value for λ is a difficult problem. Several methods have been proposed to obtain an effective choice of λ. For instance, if the norm of the error $\mathbf{e}$ on C is known, numerical results suggest that the optimal value of λ is given in Equation (67):

$$\lambda = \frac{||\mathbf{e}||^2}{||\Gamma \mathbf{w}||^2} \tag{67}$$

Equation (67) expresses the fact that the error on C must be close to the error introduced by the regularizing term [6]. If the norm of the error is not known, the most well-known methods to approximate λ are the $L-$curve method [19, 6] and the Generalized Cross-Validation (GCV) [9, 15]. The GCV method searches for the minimum of a function of λ which is an estimate of the norm of the residual. However, this method fails when the function if flat near the minimum. Because of this challenge, the L-curve method was used to estimate λ. L-curve methods consist of plotting in log-log scale the values of $||\Gamma w||$ versus $||C - Gw||$. The resulting curve is an L-shaped curve and the selected value of λ is the one corresponding to the corner of the L.

4.3. Localization of the source position. To locate the source position $\mathbf{S}_i$, we introduce the vector $\mathbf{V}^\perp = (-v_2, v_1)^T$ and the two dispersion current functions $\psi(x,y)$ and $\psi^\perp(x,y)$ defined

in an open subset O of $\mathbb{R}^2$ such that $\bar{\Omega} \subset O$ by the Equations (68) and (69):

$$D\nabla\psi + \mathbf{V} = 0 \tag{68}$$

$$\nabla\psi^{\perp} + \mathbf{V}^{\perp} = 0 \tag{69}$$

As the matrix D is invertible, setting $\psi(0,0) = \psi^{\perp}(0,0) = 0$ it follows that the two dispersion functions are given by the Equation (70):

$$\psi(x, y) = \alpha x + \beta y \quad \text{and} \quad \psi^{\perp}(x,y) = \nu_2 x - \nu_1 y \tag{70}$$

where the constants α and β are given by the Equation (71):

$$\alpha = \frac{D_{xy}\nu_2 - D_{yy}\nu_1}{\det(D)}, \quad \beta = \frac{D_{xy}\nu_1 - D_{xx}\nu_2}{\det(D)} \tag{71}$$

The following two functions in the Equation (72):

$$z(x,y,t) = e^{Rt}u(x, y) \quad \text{for} \quad u(x, y) = \{e^{\psi}, \psi^{\perp}\} \tag{72}$$

solves the adjoint Equations (73) to (76):

$$-\frac{\partial z}{\partial t} - \mathbf{V}\cdot\nabla z - \nabla\cdot D\nabla z + Rz = 0 \quad \text{in} \quad \Omega \times (0, T) \tag{73}$$

$$z(x,y,0) = 0 \quad \text{in} \quad \Omega \times (0, T) \tag{74}$$

$$z(x,y,t) = 0 \quad \text{on} \quad (\Gamma_1 \cup \Gamma_4) \times (0, T) \tag{75}$$

$$\nabla z(x,y,t) = 0 \quad \text{on} \quad \Gamma_L \times (0, T) \tag{76}$$

Multiply the Equation (17) by $z(x,y,t)$ and integrate by parts over $\Omega \times (0, T)$ with the boundary conditions Equations (18) to (20) gives the Equation (77):

$$\int_0^T \sum_{n=1}^{Ns} w_n(t) z(\mathbf{S_n}, t)\,\mathrm{dt} = \int_{\Omega} c(x,y,T)z(x,y,T)\,\mathrm{dx\,dy} + \int_0^T \int_{\Gamma_4} c[z\mathbf{V} + D\nabla z]\cdot\,\mathrm{d\Gamma\,dt} + \int_0^T \int_{\Gamma_L} cD\nabla z\cdot\,\mathrm{d\Gamma\,dt}$$

$$-\int_0^T \int_{\Gamma_1} zD\nabla c \cdot \, \mathrm{d}\Gamma \, \mathrm{dt} \tag{77}$$

where on the lateral boundary, the no-slip condition, $\mathbf{V} = 0$, have been used. By substituting $z(x,y,t) = e^{Rt}u(x,y)$ in Equation (77) and considering one point source gives the Equation (78):

$$\begin{aligned} u(\mathbf{S_n}) \int_0^T w(t)e^{Rt} \, \mathrm{dt} &= e^{RT} \int_\Omega c(x,y,T)u(x,y) \, \mathrm{dx} \, \mathrm{dy} \\ &+ \int_0^T \int_{\Gamma_4} ce^{Rt}[u\mathbf{V} + D\nabla u] \cdot \, \mathrm{d}\Gamma \, \mathrm{dt} + \int_0^T \int_{\Gamma_L} ce^{Rt} D\nabla u \cdot \, \mathrm{d}\Gamma \, \mathrm{dt} \\ &- \int_0^T \int_{\Gamma_1} e^{Rt} uD\nabla c \cdot \, \mathrm{d}\Gamma \, \mathrm{dt} \end{aligned} \tag{78}$$

The time-dependent intensity function $w_n(t)$ is known from the previous section and to locate the source position, an assumption that the integral in Equation (79) is non-zero was made.

$$\int_0^T w(t)e^{Rt} \neq 0 \tag{79}$$

By substituting $u(x,y) = \{e^{\psi}, \psi^{\perp}\}$ in the Equation (78) and using the Equations (68) and (69), gives the linear system of Equation (80):

$$\begin{cases} \alpha S_1 + \beta S_2 & = \ln\left(\dfrac{P_{e^\psi}}{P_0}\right) \\ \nu_2 S_1 - \nu_1 S_2 & = \dfrac{P_{\psi^\perp}}{P_0} \end{cases} \iff \begin{pmatrix} \alpha & \beta \\ \nu_2 & -\nu_1 \end{pmatrix} \begin{pmatrix} S_1 \\ S_2 \end{pmatrix} = \begin{pmatrix} \ln\left(\dfrac{P_{e^\psi}}{P_0}\right) \\ \dfrac{P_{\psi^\perp}}{P_0} \end{pmatrix} \tag{80}$$

where the coefficients, P_{e^ψ}, P_0 and $P_{\psi^\perp}$ in the Equation (80) are given by the Equations (81) to (83):

$$P_0 = \int_0^T w(t)e^{Rt} \, \mathrm{dt} \tag{81}$$

$$P_{e^\psi} = e^{RT} \int_\Omega e^{\psi(x,y)} c(x,y,T) \, \mathrm{dx} \, \mathrm{dy} - \int_0^T \int_{\Gamma_1} e^{Rt+\psi} D\nabla c \cdot \, \mathrm{d}\Gamma \, \mathrm{dt} \tag{82}$$

$$P_{\psi^\perp} = e^{RT}\int_{\Omega}\psi^\perp(x,y)c(x,y,T)\,\mathrm{dx}\,\mathrm{dy} + \int_0^T\int_{\Gamma_4} ce^{Rt}[\psi^\perp\mathbf{V} - D\mathbf{V}^\perp]\cdot\,\mathrm{d}\Gamma\,\mathrm{dt} - \int_0^T\int_{\Gamma_L} ce^{Rt}D\mathbf{V}^\perp\cdot\,\mathrm{d}\Gamma\,\mathrm{dt} - \int_0^T\int_{\Gamma_1} e^{Rt}\psi^\perp D\nabla c\cdot\,\mathrm{d}\Gamma\,\mathrm{dt} \tag{83}$$

Since D is invertible, the system of Equation (80) has a solution given by the Equation (84):

$$\begin{pmatrix} S_1 \\ S_2 \end{pmatrix} = \frac{1}{-\alpha\nu_1 - \beta\nu_2}\begin{pmatrix} -\nu_1 & -\beta \\ -\nu_2 & \alpha \end{pmatrix}\begin{pmatrix} \ln\left(\frac{P_{e^\psi}}{P_0}\right) \\ \frac{P_{\psi^\perp}}{P_0} \end{pmatrix} \tag{84}$$

In the following sections we implement the source identification procedure outlined so far.

5. Numerical Results and Discussion

In this section, we carry out numerical experiments in the case of a rectangular domain defined by the Equation (85):

$$\Omega = \{(x,y) \text{ such that } \quad 0 < x < L \quad \text{and} \quad 0 < y < H\} \tag{85}$$

For the numerical computation, the domain $\Omega \times (0,T)$ is scaled up according to the non-dimensional variables in the Equation (86):

$$\begin{cases} \tilde{x} = \dfrac{x}{L}, \tilde{t} = \dfrac{t}{t_c},\ \tilde{y} = \dfrac{y}{L}, \tilde{S}_i = \dfrac{a_i}{L}, \tilde{\mathbf{V}} = \dfrac{\mathbf{V}}{v}, \\ \tilde{D} = \dfrac{D}{D_c}, \tilde{C} = \dfrac{C}{C_c}, \tilde{R} = Rt_c,\ \tilde{F} = f_c\sum_{i=1}^N \tilde{w}(t)\delta(\tilde{x} - \tilde{S}_i) \end{cases} \tag{86}$$

Substituting the variables in Equation (86) in the Equations (17) to (19) gives the Equations (87), (89) and (90).

$$\frac{C_c}{t_c}\frac{\partial\tilde{C}}{\partial\tilde{t}} + \frac{VC_c}{L}\tilde{\mathbf{V}}\cdot\tilde{\nabla}\tilde{C} - \frac{C_cD_c}{L^2}\tilde{\nabla}\cdot(\tilde{D}\tilde{\nabla}\tilde{C}) + \frac{\tilde{R}C_c}{t_c}\tilde{C} = f_c\sum_{i=1}^N \tilde{w}(t)\delta(\tilde{x} - \tilde{S}_i) \tag{87}$$

$$\tilde{C}(\tilde{x},\tilde{y},0) = 0 \quad \text{in} \quad \Omega \tag{88}$$

$$\tilde{C}(\tilde{x},\tilde{y},\tilde{t}) = 0 \quad \text{on} \quad \partial\Omega \tag{89}$$

$$\tilde{\nabla}\tilde{C}(\ell,\tilde{y},\tilde{t}) = 0 \quad \text{on} \quad \partial\Omega \tag{90}$$

Multiply the Equation (87) by t_c/C_c gives the Equation (91):

$$\frac{\partial \tilde{C}}{\partial \tilde{t}} + \frac{Vt_c}{L}\tilde{\mathbf{V}}\cdot\tilde{\nabla}\tilde{C} - \frac{t_c D_c}{L^2}\tilde{\nabla}\cdot(\tilde{D}\tilde{\nabla}\tilde{C}) + \tilde{R}\tilde{C} = \frac{f_c t_c}{C_c}\sum_{i=1}^{N}\tilde{w}(t)\delta(\tilde{x}-\tilde{S}_i) \tag{91}$$

The choice of the coefficient t_c is based on the convective transport, that is, $t_c = L/V$, which is the characteristic time it takes to transport a signal by convection through the domain. Also as the convection term dominates over the diffusion term. Meanwhile, C_c is carefully chosen to make the coefficient in the source term unity, that is, $C_c = t_c f_c = L f_c/V$. This gives the Equation (92);

$$\frac{\partial \tilde{C}}{\partial \tilde{t}} + \tilde{\mathbf{V}}\cdot\tilde{\nabla}\tilde{C} - \frac{1}{Pe}\tilde{\nabla}\cdot(\tilde{D}\tilde{\nabla}\tilde{C}) + \tilde{R}\tilde{C} = \sum_{i=1}^{N}\tilde{w}(t)\delta(\tilde{x}-\tilde{S}_i) \tag{92}$$

where Pe is the Peclet number. The Peclet number measures the ratio of the convection and the diffusion terms, that is, the Equation (93).

$$Pe = \mathrm{Pe} = \frac{\text{convection}}{\text{diffusion}} = \frac{VL}{D_c} \tag{93}$$

5.1. Numerical tests and discussion. In this subsection, we use the established identification method to carry out some numerical experiments. To this end, we employ in Equation (92) the coefficients in the Equation (94) :

$$L = 2500m,\ a_T = 10m,\ a_L = 0.2,\ R = 10^{-5}s^{-1} \tag{94}$$

To identify the elements S and $w(t)$ defining the source occurring in the controlled portion of a an aquifer represented by the segment $(0,L)$. We assume controlling this portion of a aquifer for $T = 4h$. To generate the records $C(a,t)$ and $C(b,t)$ at the two observation points a and b, we solve the problem Equation (92) using the finite volume method with the source located at $(900m, 10m)$ loading the following time-dependent intensity function in the Equation (95):

$$w(t) = \sum_{i=1}^{3} b_i e^{-u_i(t-q_i)^2} \tag{95}$$

where $b_1 = 1.2$, $b_2 = 0.4$, $b_3 = 0.6$, $u_1 = 10^{-6}$, $u_2 = 5\times10^{-5}$, $u_3 = 10^{-6}$, $q_1 = 4.5\times10^3$, $q_2 = 6.5\times10^3$, $q_3 = 9\times10^3$.

Over the whole control time T, we employ 100 measures of C at each of the two observation points a and b. Those measures have been taken at the regularly distributed discrete times with equal time steps. As far as the source position $S = (Sx, Sy)$ is concerned, we employ the approximation of the Dirac mass in the Equation (96) [12];

$$\delta(x - Sx, y - Sy) \approx \left(\frac{1 + \cos(\pi(x - Sx))}{2\varepsilon}\right)\left(\frac{1 + \cos(\pi(y - Sy))}{2\varepsilon}\right) \tag{96}$$

We set the parameter, $\varepsilon = 10^{-5}$ in Equation (96). Then, to apply the identification method established in the previous section, we start by computing the intensity function as outlined in Section 4.1 after which we apply the Tikhonov Regularization method as outlined in Section 4.2. For the L-curve method, we use $\lambda = \{e^{-4}, e^{-5}, e^{-3}\}$. After the identification of the intensity, we compute the three integrals in Equations (81) to (83) involving the unknown data $C(x, y, T)$. We end by using the computed integrals to solve the system of Equation (84). We present the recovered solution with the three values of the regularization parameter in Figures 2, 4 and 6 alongside the forward solutions in Figures 3, 5 and 7 respectively:

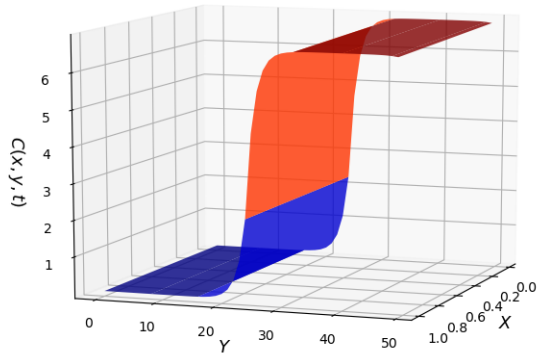

FIGURE 2. Recovered Solution State with the regularization parameter $\lambda = e^{-4}$

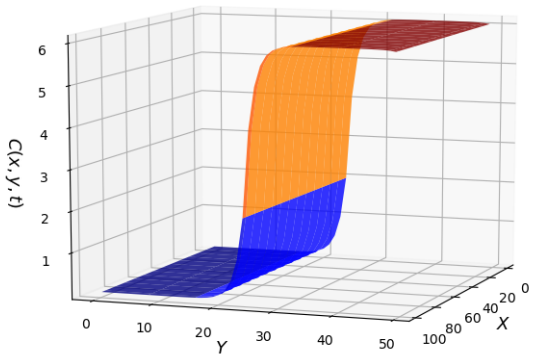

FIGURE 3. The Forward Problem

Table 1 gives the percentage error obtained on obtaining the intensity function with the regularization parameter of $\lambda = e^{-4}$.

TABLE 1. Percentage Error on the Recovered Solution with Regularization Parameter $\lambda = e^{-4}$

	Forward Solver	Recovered Data	Percentage Error
1.0	9.028393e-08	1.017928e-07	0.000001
2.0	1.393656e-07	1.571341e-07	0.000002
3.0	2.639602e-07	2.976115e-07	0.000003
4.0	5.316652e-07	5.994507e-07	0.000007
5.0	1.087668e-06	1.226304e-06	0.000014
6.0	2.233487e-06	2.518223e-06	0.000028
7.0	4.590483e-06	5.175916e-06	0.000059
8.0	9.436815e-06	1.063969e-05	0.000120
9.0	1.940056e-05	2.187378e-05	0.000247
10.0	3.988490e-05	4.496968e-05	0.000508
11.0	8.199811e-05	9.245257e-05	0.001045
12.0	1.685775e-04	1.900759e-04	0.002150
13.0	3.465734e-04	3.907368e-04	0.004416
14.0	7.125100e-04	8.033370e-04	0.009083
15.0	1.464828e-03	1.651617e-03	0.018679

As from Table 1, the percentage error is very small so we conclude the method with $\lambda = e^{-4}$ has worked perfectly.

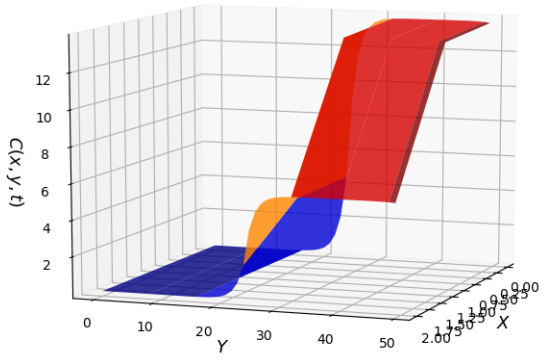

FIGURE 4. Recovered Solution State with the regularization parameter $\lambda = e^{-5}$

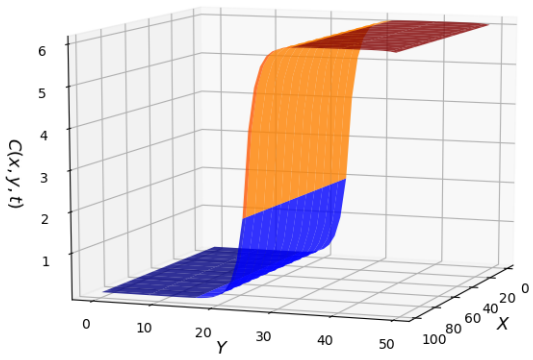

FIGURE 5. Forward Solution

Table 2 gives the percentage error obtained on obtaining the intensity function with the regularization parameter of $\lambda = e^{-5}$.

TABLE 2. Percentage Error on the Recovered Solution with Regularization Parameter $\lambda = e^{-5}$

	Forward Solver	Recovered Data	Percentage Error
1.0	9.028393e-08	3.899311e-08	0.000005
2.0	1.393656e-07	6.019122e-08	0.000008
3.0	2.639602e-07	1.140029e-07	0.000015
4.0	5.316652e-07	2.296231e-07	0.000030
5.0	1.087668e-06	4.697574e-07	0.000062
6.0	2.233487e-06	9.646299e-07	0.000127
7.0	4.590483e-06	1.982603e-06	0.000261
8.0	9.436815e-06	4.075705e-06	0.000536
9.0	1.940056e-05	8.378993e-06	0.001102
10.0	3.988490e-05	1.722605e-05	0.002266
11.0	8.199811e-05	3.541452e-05	0.004658
12.0	1.685775e-04	7.280767e-05	0.009577
13.0	3.465734e-04	1.496830e-04	0.019689
14.0	7.125100e-04	3.077289e-04	0.040478
15.0	1.464828e-03	6.326509e-04	0.083218

As from Table 2, the percentage error is very small but the recovered intensity function is not very close to the initial intensity this is due to stability of the method. For practical purposes, the value of the regularization parameter to use would be $\lambda = e^{-4}$. we test $\lambda = e^{-3}$ on Figure 6.

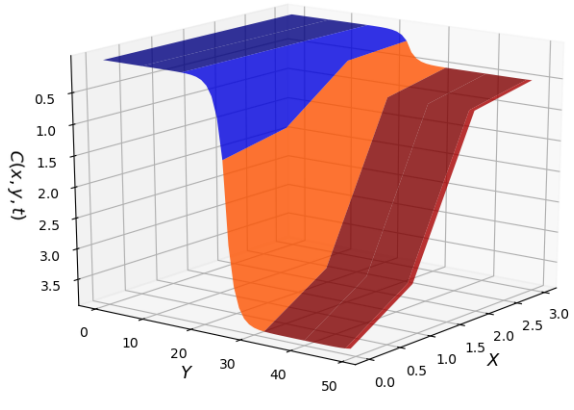

FIGURE 6. Recovered Solution State with the regularization parameter $\lambda = e^{-3}$

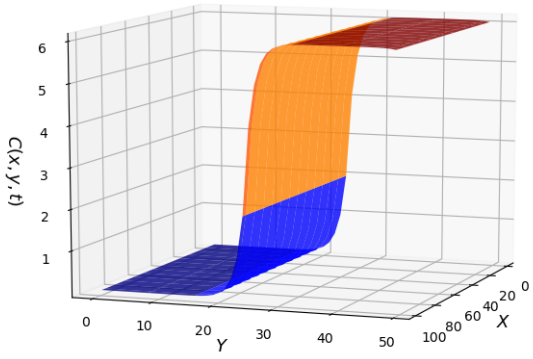

FIGURE 7. Forward Solution

The Table 2 gives the percentage error obtained on obtaining the intensity function with the regularization parameter of $\lambda = e^{-3}$.

TABLE 3. Percentage Error on the Recovered Solution with Regularization Parameter $\lambda = e^{-3}$

	Forward Solver	Recovered Data	Percentage Error
1.0	9.028393e-08	4.295685e-08	0.000005
2.0	1.393656e-07	6.633736e-08	0.000007
3.0	2.639602e-07	1.256901e-07	0.000014
4.0	5.316652e-07	2.530473e-07	0.000028
5.0	1.087668e-06	5.179344e-07	0.000057
6.0	2.233487e-06	1.062585e-06	0.000117
7.0	4.590483e-06	2.185058e-06	0.000241
8.0	9.436815e-06	4.489853e-06	0.000495
9.0	1.940056e-05	9.233444e-06	0.001017
10.0	3.988490e-05	1.898277e-05	0.002090
11.0	8.199811e-05	3.904438e-05	0.004295
12.0	1.685775e-04	8.020278e-05	0.008837
13.0	3.465734e-04	1.649876e-04	0.018159
14.0	7.125100e-04	3.392491e-04	0.037326
15.0	1.464828e-03	6.972958e-04	0.076753

According to Tables 1 to 3 clearly, the optimal value of the regularization parameter we to use in determining source position is $\lambda = e^{-4}$ since the other values bring instabilities. To locate the source position, we use the values of C to compute the integrals in Equations (81) to (83) and use the result to solve the system Equation (80). Table 4, presents some numerical results obtained from the localization of a source

TABLE 4. Recovered Source Positions

	x position	y position	recovered x	recovered y
1.0	10.0	150.0	11.803534	197.805191
2.0	20.0	140.0	18.815498	143.311173
3.0	30.0	130.0	36.827462	138.817155
4.0	40.0	120.0	42.839426	114.323136
5.0	50.0	110.0	54.851390	119.829118
6.0	60.0	100.0	58.038751	99.422799
7.0	70.0	90.0	76.360121	103.583484
8.0	80.0	80.0	68.681490	69.744169
9.0	90.0	70.0	94.002860	81.904853
10.0	100.0	60.0	133.324229	70.065538
11.0	110.0	50.0	145.645599	58.226223
12.0	120.0	40.0	137.966968	49.386908
13.0	130.0	30.0	132.288338	34.547592
14.0	140.0	20.0	122.609707	23.708277

The numerical results presented in Table 4 show that the source localization procedure established enables us to identify the source position with relatively good accuracy. The observed error on the localized source position is due to the boundary records are not generated by a point source that is the Dirac mass but rather by its approximation given in Equation (96) and an approximation of the integrals Equations (81) to (83) introduces errors.

6. CONCLUSION

In this study, a solution for an inverse source problem of identifying multiple unknown time-dependent point sources occurring in the two-dimensional ADRE was developed. Validation of the model was demonstrated by using hypothetical examples as there was no groundwater data in the literature. To generate the hypothetical data FVM was used to solve the forward problem and approximation made at discreet points. Numerical experiments on the BOD data were carried out. The obtained numerical results show that the developed identification method is accurate. In this paper, we only considered the transport of the pollutant in the groundwater without considering groundwater flow. An outlook for the results established in the present study is their extension towards at least the following directions: Firstly, incorporating groundwater flow equations for the transport of groundwater, ADRE for the transport of the pollutants and solitary

vibrations available on the interaction between groundwater and surface water. Secondly, apply the developed identification method using other reference geometries and real-life measurements taken on a flow crossing a monitored domain of arbitrary geometric shape. Thirdly, treat the three-dimensional case for the ADRE. Finally, apply the developed methodology into other applications.

ACKNOWLEDGMENT

This work was supported by Pan African University Institute for Basic Sciences Technology and Innovation (PAUSTI) for which the authors express their sincere gratitude. We also thank Dr. Mark Kimathi for his valuable comments and help.

CONFLICT OF INTERESTS

The author(s) declare that there is no conflict of interests.

REFERENCES

[1] Hamdi Adel. A non-iterative method for identifying multiple unknown time-dependent sources compactly supported occurring in a 2d parabolic equation. Inverse Probl. Sci. Eng. 26 (5) (2018), 744–772.

[2] American Public Health Association, American Water Works, Water Pollution Control Federation, and Water Environment. Standard methods for the examination of water and wastewater volume 2. American Public Health Association, 1915.

[3] Richard C Aster, Brian Borchers, and Clifford H Thurber. Parameter estimation and inverse problems. Elsevier, 2018.

[4] Jacob Bear and Yehuda Bachmat. Introduction to modeling of transport phenomena in porous media volume 4. Springer Science & Business Media, 2012.

[5] Claude Brezinski, Michela Redivo-Zaglia, Giuseppe Rodriguez, and Sebastiano Seatzu. Extrapolation techniques for ill-conditioned linear systems. Numer. Math. 81 (1) (1998), 1–29.

[6] Claude Brezinski, Giuseppe Rodriguez, and Sebastiano Seatzu. Error estimates for linear systems with applications to regularization. Numer. Algorithms 49 (1-4) (2008), 85–104.

[7] Claude Brezinski, Giuseppe Rodriguez, and Sebastiano Seatzu. Error estimates for the regularization of least squares problems. Numer. Algorithms 51 (1) (2009), 61–76.

[8] JR Cannon. Determination of an unknown heat source from overspecified boundary data. SIAM J. Numer. Anal. 5 (2) (1968), 275–286.

[9] P Carven and G Wahba. Smoothing noisy data with spline functions: estimationg the correct degree of smoothing by the method of generalized cross-validation. Numer. Math. 31 (1979), 377–403.

[10] William E Dobbins. Bod and oxygen relationship in streams. J. Sanitary Eng. Division 90 (3) (1964), 53–78.

[11] Abdellatif El Badia and Tuong Ha-Duong. On an inverse source problem for the heat equation. application to a pollution detection problem. J. Inverse Ill-Posed Probl. 10 (6) (2002), 585–599.

[12] Björn Engquist, Anna-Karin Tornberg, and Richard Tsai. Discretization of dirac delta functions in level set methods. J. Comput. Phys. 207 (1) (2005), 28–51.

[13] Martin Fuhry and Lothar Reichel. A new tikhonov regularization method. Numer. Algorithms 59 (3) (2012), 433–445.

[14] Richard Garduño. India groundwater governance case study. Water Papers, 2011.

[15] Gene H Golub, Michael Heath, and Grace Wahba. Generalized cross-validation as a method for choosing a good ridge parameter. Technometrics, 21 (2) (1979), 215–223.

[16] Gene H Golub, Per Christian Hansen, and Dianne P O'Leary. Tikhonov regularization and total least squares. SIAM J. Matrix Anal. Appl. 21 (1) (1999), 185–194.

[17] Jacques Hadamard. Sur les problèmes aux dérivées partielles et leur signification physique. Princeton university bulletin pages 49–52, 1902.

[18] Adel Hamdi. Detection and identification of multiple unknown time-dependent point sources occurring in 1d evolution transport equations. Inverse Probl. Sci. Eng. 25 (4) (2017), 532–554.

[19] Per Christian Hansen and Dianne Prost O'Leary. The use of the l-curve in the regularization of discrete ill-posed problems. SIAM J. Sci. Comput. 14 (6) (1993), 1487–1503.

[20] Linxian Huang, Lichun Wang, Yongyong Zhang, Liting Xing, Qichen Hao, Yong Xiao, Lizhi Yang, and Henghua Zhu. Identification of groundwater pollution sources by a sce-ua algorithm-based simulation/optimization model. Water, 10 (2) (2018), 193.

[21] Diederik Johannes Korteweg and Gustav De Vries. On the change of form of long waves advancing in a rectangular canal. The London, Edinburgh, and Dublin Philosophical Magazine and Journal of Science, 39 (240) (1895), 422–443.

[22] Cornelius Lanczos. Linear differential operators volume 18. SIAM, 1997.

[23] Zeng Lingjie and Zhang Xu. Probability-based inverse characterization of the instantaneous pollutant source within a ventilation system. Build. Environ. 143 (2018), 378 – 389.

[24] Peter Linz. Numerical methods for volterra integral equations of the first kind. Computer J. 12 (4) (1969), 393–397.

[25] Jacques-Louis Lions. Pointwise control for distributed systems. Control and Estimation in Distributed Parameter Systems, H, T. Banks ed., SIAM, Philadelphia, pages 1–39, 1992.

[26] Pooran S Mahar and Bithin Datta. Identification of pollution sources in transient groundwater systems. Water Resources Manage. 14 (3) (2000), 209–227.

[27] Imed Mahfoudhi. Problèmes inverses de sources dans des équations de transport à coefficients variables. PhD thesis, Rouen, INSA, 2013.

[28] Mehdi Mazaheri, Jamal Mohammad Vali Samani, and Hossein Mohammad Vali Samani. Mathematical model for pollution source identification in rivers. Environ. Forensics 16 (4) (2015), 310–321.

[29] Serena Morigi, Lothar Reichel, and Fiorella Sgallari. A truncated projected svd method for linear discrete ill-posed problems. Numer. Algorithms, 43 (3) (2006), 197–213.

[30] Alan C Newell. Solitons in mathematics and physics volume 48. Siam, 1985.

[31] Akira Okubo. Diffusion and ecological problems:(mathematical models). Biomathematics, 1980.

[32] JB Passioura. Hydrodynamic dispersion in aggregated media: 1. theory. Soil sci. 111 (6) (1971), 339–344.

[33] Lothar Reichel and Qiang Ye. Simple square smoothing regularization operators. Electron. Trans. Numer. Anal. 33 (2009), 63-83.

[34] Jean-Claude Saut and Bruno Scheurer. Unique continuation for some evolution equations. J. Differential Equations 66 (1) (1987), 118–139.

[35] M Yamamoto. Conditional stability in determination of force terms of heat equations in a rectangle. Math. Computer Model. 18 (1) (1993), 79–88.